A simple qualitative description of EMC ratios μ^A for $0.2 \lesssim x \lesssim 1.5$ and some sample calculations.

A.S. Rinat and M.F. Taragin

Weizmann Institute of Science, Department of Particle Physics, Rehovot 76100, Israel

M. Viviani

INFN, Sezione Pisa and Phys. Dept., University of Pisa, I-56100, Italy
(Dated: February 9, 2008)

We study EMC ratios on the basis of a relation between Structure Functions (SF) for a nucleus and for a nucleon, which is governed by a SF $f^{PN,A}(x,Q^2)$ of an unphysical nucleus, composed of point-nucleons. We demonstrate that the characteristic features of EMC ratios μ^A are determined by the above $f^{PN,A}$ and the SF of free nucleons. We account for the positions of the points $x_{1,2}$ in the interval $0.2 \lesssim x \lesssim 0.9$, where $\mu^A(x,Q^2)=1$ and also for the minimum x_m in that interval. We similarly describe the oscillations in μ^A for $Q^2 \lesssim (3.5-4.0)\,\mathrm{GeV}^2$ in the Quasi-Elastic peak region $0.95 \lesssim x \lesssim 1.05$ and for its subsequent continuous increase up to $x \approx 1.4$. Finally we compute μ^A over the entire range above for $A = {}^4\mathrm{He}$, C, Fe and Au and several Q^2 values. The results are in reasonable agreement with both directly measured and indirectly extracted data.

The literature on the EMC effect reads like some late 19th century trilogy. Although spun out over hundreds of pages, some vague plot just does not reach a relieving resolution.

I. INTRODUCTION.

After the first measurements some 20 years ago, a keen interest developed in understanding EMC ratios $\mu^A(x,Q^2) = F_2^A(x,Q^2)/F_2^D(x,Q^2)$ of Structure Functions (SF) per nucleon of any target A and of the D (x is the Bjorken variable $0 \leq x = Q^2/2M\nu \leq A$; ν, Q^2 are the energy loss and minus the squared 4-momentum transfer; M is the nucleon mass). Over the years, re-analysis of older data and a generation of new experiments have been performed, the latter frequently at much larger Q^2 and often down to very small x. Disregarding the range $x \lesssim 0.20$, in all EMC experiments with in parallel measured F_2^A, F_2^D, the Bjorken variable x lies in the 'classical' EMC regime $0.2 \lesssim x \lesssim 0.9$. The canon of direct experiments was closed some 10 years ago. Refs. [1, 2] report on the status up to about a decade ago.

Indirect information on $\mu^A(x \gtrsim 0.9)$ comes from separately measured inclusive cross sections on targets A and on D. Before 1999 all extractions of their ratios for $x \gtrsim 0.9$ have been for relatively low Q^2. [3, 4, 5]. Refs. [6, 7], [8] and [9] contain data for, respectively, ^{3}He, $A \geq 4$ (SLAC NE3 experiment) and on Al. D data for more or less the same kinematics are from Refs. [10, 11, 12]. Below we shall exploit the more recent JLab E89-008 experiment for the extraction of EMC ratios at substantially larger Q^2 from data on several targets A [13, 14] and on D [14, 15]. Finally we mention the Drell-Yan process as an additional source of information (see for instance Ref.[16]).

The combined pools of information lead to the following observations:

i) In the classical regime $0.2 \lesssim x \lesssim 0.9$, $|1 - \mu^A(x,Q^2)|$ hovers between ≈ 0 and 0.15-0.20 with little A or Q^2 dependence.

ii) In the adjacent range $0.95 \lesssim x \lesssim 1.05$ around the quasi-elastic (QE) point $x = 1$, extracted EMC ratios for $Q^2 \lesssim 3.5\,\mathrm{GeV}^2$ show a sharp rise, followed by an abrupt decrease toward minima around $x \approx 1$, the depth of which depends on A and Q^2.

iii) In the 'deep' quasi-elastic (DQE) region $1.05 \lesssim x \lesssim 1.4$, immediately beyond the range ii), EMC ratios resume the rise mentioned in ii) with a slope increasing with Q^2. Those ratios reach maxima of the order 4-7 and level off, eventually. The very small, and increasingly imprecise composing $F_2^{A,D}$ cause considerable experimental scatter in μ^A for the largest x.

Attempts to understand the above observations [1, 2] concentrated primarily on the classical range, where the preferred tool of analysis has been the Plane Wave Impulse Approximation (PWIA) [17, 18, 19, 20]. Different versions did not converge onto an unanimously accepted understanding. Some authors conclude that the crucial ingredients in the PWIA, namely Fermi averaging and binding corrections, do not account for the data (see, for instance, Refs. [21, 22]), while others reach the opposite conclusions [20, 23, 24]. From that rather frustrating situation sprang alternative, and occasionally far-flung approaches. We mention the use of Bethe-Salpeter equations for nuclear vertex functions or bound state wave functions [25], medium modifications of nucleons [22], the introduction of, in the EMC field, exotic chiral solitons [21] and more.

For two reasons it seems timely to-reopen the nearly stalled discussion. First, a new inclusive scattering experiment

JLab E03-103 is currently running on D, ^{3}He and ^{4}He targets [26]. We shall soon have sorely missing accurate EMC data on ^{3}He and ^{4}He, covering a wide range of x which cross the QE point $x = 1$. Those will be of special interest, because for the lightest nuclei, EMC ratios differ from the mainstream of heavier targets, among which the A-dependence ot those ratios is sizably weaker. Moreover, only for the former class of nuclei can one perform accurate calculations.

The second reason is the recurrently expressed wish for a simple, qualitative understanding of EMC ratios. Here one is warned against pitfalls of over-simplification, for instance in attempts to understand the steeply rising μ^A, setting in at $x \approx 0.9$. Off-hand one expects $F_2^D(x \lesssim 1)$ to become very small. In fact, the SF F_2^D for two non-interacting component nucleons vanishes for $x = 1$, and one does not expect binding effects to be significant. The above is correct, but a similar, and even more pronounced effect occurs for SFs of all heavier targets. As a result, deep *minima*, and not maxima occur in EMC ratios at $x = 1$.

In spite of the above skepsis, we shall attempt below such a description, invoking a relation between nuclear and nucleonic SFs, which is mediated by a SF $f^{PN,A}$ of a fictitious nucleus, composed of point-nucleons [27]. That SF is a covariant generalization [28] of a similar one in the non-relativistic Gersch-Rodriguez-Smith (GRS) theory for inclusive scattering [29]. It implicitly contains the equivalent of Fermi-averaging and binding effects, which are the emphasized ingredients of the PWIA, and goes beyond it: it enables a relatively simple computation of the dominant Final State Interaction (FSI).

The above covariant GRS approach has been successfully applied to an extensive body of inclusive scattering data with $Q^2 \gtrsim (2.5 - 3.0)$ GeV^2 [30, 31, 32, 33] and to observables, related to nuclear SF F_k^A [34]. It is thus natural to study EMC ratios in that approach. Actually, a first version of the model has years ago been shown to reasonably account for the measured μ^{Fe} in the classical region [31].

This note is organized as follows:

1) We re-state the relation between nuclear and nucleon SF by means of $f^{PN,A}$ and list distinct properties of the latter.

2) We demonstrate that virtually all features of EMC ratios F_2^A/F_2^d in the entire range of our interest $0.20 \lesssim x \lesssim 1.50$ can be qualitatively understood from the x, Q^2, and in particular from the outspoken A dependence of the above SF $f^{PN,A}$. In the 'classical' EMC regime $0.20 \lesssim x \lesssim 0.90$ those characteristics are the positions of the points $x_{1,2}$, where the EMC ratios cross the value 1, including the A-dependence of x_2 and the approximate position of an intermediate minima. In addition, we describe how for $Q^2 \lesssim (3-4)$ GeV^2 a sharp rise in μ^A, setting in for $x \approx 0.9$, abruptly turns into a deep minimum close to $x = 1$, and continues its rise for $x \gtrsim 1.05$ in a Q^2-dependent fashion. For increasing $Q^2 \gtrsim (4 - 5)$ GeV^2 the above minima degenerate into some minor structure.

3) In support of the above qualitative considerations, we present results for actual calculations and compare those with directly measured and extracted EMC data.

4) In conclusion we compare our approach with an approximatively equally successful, but less transparent, Distorted Wave Impulse Approximation (DWIA) description.

II.   GENERALITIES.

We start with a previously postulated relation between SF $F_k^{N,A}$ for nucleons ($N = p, n$) and a nucleus [27, 28]

$$F_2^A(x, Q^2)(\equiv F_2^{A,\delta N}(x, Q^2)) = \int_x^A dz f^{PN,A}(z, Q^2) F_2^{\langle N \rangle}\left(\frac{x}{z}, Q^2\right) , \tag{2.1}$$

$$= \int_{1/A}^{1/x} du B^A(u, Q^2) F_2^{\langle N \rangle}(xu, Q^2) , \tag{2.2}$$

with

$$B^A(u, Q^2) = f^{PN,A}(1/u, Q^2)/u^2 , \tag{2.3}$$

In both forms the integrands separate x and A dependence. Above we use a weighted p, n nucleon SF with δN the neutron excess. Thus

$$F_2^{\langle N \rangle} = \frac{F_2^n + F_2^p}{2} + \frac{\delta N}{2A}(F_2^n - F_2^p) , \tag{2.4}$$

The connection between the nuclear and averaged nucleon SF above is provided by $f^{PN,A}$, which is the SF of a fictitious target A, composed of point-nucleons.

The relations (2.1) and (2.2) are exact in the Bjorken limit and have empirically been shown to hold for finite $Q^2 \geq Q_0^2 \approx (2.0 - 2.5)\,\mathrm{GeV}^2$ [32, 35]. Also the PWIA for F_2^A is of the form (2.1) with $f \rightarrow f^{PWIA}$.

Eqs. (2.1) and (2.2) describe partons which originate exclusively from nucleons. The same from virtual bosons [36], as well as (anti-)screening effects [37], are negligible for $x \gtrsim 0.2$; we shall restrict ourselves to that region. Finally, in view of the relatively high Q^2 involved, one may neglect the mixture of F_1^N in the integrand in Eq. (2.1) [38, 39].

It will be useful to separate $F^{\langle N \rangle} = F^{\langle N \rangle, NE} + F^{\langle N \rangle, NI}$ into components NE, NI, which correspond to processes in which the nucleon absorbs the exchanged virtual photon elastically ($\gamma^* + N \rightarrow N$) or inelastically ($\gamma^* + N \rightarrow$ hadrons, partons). For our purposes it suffices to recall that $F_2^{\langle N \rangle, NE} = \delta(1 - x)\mathcal{G}_2(Q^2)$, with $\mathcal{G}_2(Q^2)$ some linear combination of squared static nucleon form factors. Substitution of the above into Eqs. (2.1) trivially produces for the corresponding NE part of any nuclear SF

$$F_2^{A,NE}(x, Q^2) = f^{PN,A}(x, Q^2)\mathcal{G}_2(Q^2) . \tag{2.5}$$

The above SF $f^{PN,A}$ are constructed from many-body target density matrices, which are diagonal in all except one coordinate. Those can only be calculated with precision for the lightest nuclei, $A \leq 4$. The computation of $f^{PN,A}$ requires in addition information on (off-shell) NN scattering (see for instance Ref. 31).

We summarize salient properties of the SF $f^{PN,A}$ [34]:

a) The normalized SFs $f^{PN,A}(x, Q^2)$ are smooth functions of x and are approximately symmetric around a, Q^2-dependent maximum $x_M^A(Q^2) \approx 1$, close to the QE peak (Fig. 1). We note from Eqs. (2.1) and (2.2) that the A-dependence of nuclear SFs is largely governed by the same in $f^{PN,A}$.

b) For given Q^2, peak-values of $f^{PN,A}$ strongly decrease with increasing A from D, He to general A, and show only few % differences between nuclei with $A > 12$. Due to normalization, also their widths show marked variations with $A < 12$ (Fig. 1).

c) The above peak-values increase with Q^2 (see Figs. 2 and 3) and reach rather slowly an asymptotic limit.

d) Ratios of peak values $f^{PN,A}(x \approx 1, Q^2)/f^{PN,A'}(x \approx 1, Q^2)$ are only weakly Q^2-dependent.

The above properties of $f^{PN,A}$ determine those of B^A, Eq. (2.3), which in Figs. 4 and 5 are displayed for a few targets and for $Q^2 = 3.5, 10\,\mathrm{GeV}^2$. B^A obviously peaks around $u \approx 1$. It decreases on both sides with increasing $|1 - u|$, and due to the factor $1/u^2$ in its definition (2.3), in a more asymmetric fashion than does $f^{PN,A}$. In the following, we use $\bar{A}$ to specify a generic target with $A \geq 12$. Inspection of Figs. 4 and 5 shows that the various $B^{\bar{A}}$ intersect B^D at $u_i \approx 0.9$ and 1.1, while B^D and $B^{^4\mathrm{He}}$ cross at values slightly closer to 1. The above enables B^A to be ordered as function of A. Practically independent of Q^2 one has

$$B^D > B^{^4\mathrm{He}} > B^{\bar{A}} , \quad 1.1 \gtrsim u \gtrsim 1.0 , \tag{2.6}$$

$$B^D \ll B^{^4\mathrm{He}} \approx B^{\bar{A}} , \quad u \lesssim 0.9 , u \gtrsim 1.1 . \tag{2.7}$$

More details on B^A and other functions to be mentioned are entered in Table I.

III. CHARACTERISTIC FEATURES OF EMC RATIOS.

Unless stated otherwise, we focus on the usually dominant NI parts of both SFs in EMC ratios.

A. The classical range $0.2 \lesssim x \lesssim 0.90$.

I) It is an experimental fact, that the slope of $F_2^{p,D}(x, Q^2)$, which varies smoothly as function of Q^2, vanishes for $x_1 \approx 0.18 - 0.20$ (see for instance Ref. [40]). Since also the x-derivative of those functions around that x is small, standard reasoning justifies in the neighborhood of x_1 the 'primitive' determination [18, 41]

$$F_2^n(x, Q^2) \approx 2F_2^D(x, Q^2) - F_2^p(x, Q^2) . \tag{3.1}$$

Using the above in Eq. (2.4), one has in that x region $F_2^D \approx F_2^p \approx F_2^n \approx F_2^{\langle N \rangle}$. Next, from Eqs. (2.1), (3.1) and property a) in Section II, one extracts for any A approximate information on the *nucleonic* components of nuclear SFs and their derivatives. For $x' < x_0 \approx 0.18 \ll x \approx 1$ and independent of A, one finds

$$F_2^A(x', Q^2) = \int_{x'}^{A} dz\, f^{PN,A}(z, Q^2) F_2^{\langle N \rangle}\left(\frac{x'}{z}, Q^2\right) ,$$

$$\approx F_2^{\langle N \rangle}(x', Q^2) \int_0^A dz f^{PN,A}(z, Q^2) \ ,$$

$$= F_2^{\langle N \rangle}(x', Q^2) \ , \tag{3.2}$$

$$\frac{\partial F_2^A(x', Q^2)}{\partial x'} \approx \frac{\partial F_2^{\langle N \rangle}(x', Q^2)}{\partial x'} \ , \tag{3.3}$$

Strictly speaking, Eqs. (3.2), (3.3) hold for $x' = 0$. However, the nucleonic parts of $F_2^{\langle N \rangle}(x')$ and $\partial F_2^{\langle N \rangle}(x')/\partial x'$ hardly change up to $x' \lesssim x_0$, hence for those sufficiently small x_1, and independent of A and Q^2, $\mu^A(x_1 \approx (0.18-0.20), Q^2) \approx 1$. This is indeed observed for all EMC data [1, 42].

II) Next we consider the interval $x_1 \lesssim x \lesssim 1$ and focus on the integrand of Eq. (2.2), i.e. the product of the A-dependent $B^A(u, Q^2)$ and the weighted nucleon SF $F_2^{\langle N \rangle}(xu, Q^2)$. The former is dominated by the peak region $u \approx 1$, while $F_2^{\langle N \rangle}$ smoothly decreases with increasing argument xu, and is practically negligible for $xu \gtrsim 0.80$ (we shall return below to the physical NE boundary $x = 1$).

Whereas the above mentioned ordering in A of $B^A(u)$ depends only on u, the same for its product with $F_2^{\langle N \rangle}$, and thus of the integral F_2^A, Eq. (2.1), is crucially influenced by x, for instance in the deep inelastic (DI) x-range $0.2 \lesssim x \lesssim 0.8$. There the argument xu of $F_2^{\langle N \rangle}$ in the u−integral (2.2) is usually $\lesssim 0.8$ in regions around $u \approx 1$, where B^A is large. The above-mentioned A-dependence of B^A then allows the prediction

$$\mu^{\bar{A}} < \mu^{^4\text{He}} < 1 \ , \qquad 0.2 \lesssim x \lesssim 0.8 \ . \tag{3.4}$$

In order to obtain non-negligible $F_2^{\langle N \rangle}(xu)$ for increasing $x \gtrsim 0.8$ one needs $u < 1$, ($x > 1$ or equivalently $\nu < \nu_{\text{QEP}}$). Those u are on the elastic, lower u side of the peak, where B^A is appreciably smaller than at the peak. Fig. 6 illustrates the above for $B^A(u)F_2^{\langle N \rangle}(xu)$ for He, Fe and Au: in each step between the sample values $x = 0.15, 0.5, 0.85, 1.2$, the above product drops by roughly a factor 10.

Returning to the EMC ratios, we already established that on the elastic side $u < 1$ of the peak, the functions B^A are ordered as $B^D < B^{^4\text{He}} \approx B^{\bar{A}}$ (see also Table I) and therefore expect that

$$\mu^{^4\text{He}} \approx \mu^{\bar{A}} > 1 \ , \qquad 0.85 \lesssim x \lesssim 0.95 \ . \tag{3.5}$$

As x grows, the contributing u-region tends to contract to small values of u, where $B^D \ll B^A$ and therefore $\mu^A \gg 1$. We emphasize, that the understanding of the presented orderings do not require precise values for the frequently very small values of the involved nuclear SF, but derive from well-defined, qualitative features of $B^A(u, Q^2)$ (i.e. on $f^{PN,A}(x, Q^2)$) and from the simple functional behavior of $F_2^{\langle N \rangle}(xu, Q^2)$.

III) From the inequalities (3.4), (3.5) and the smoothness of all factors in the integrand, one predicts a second intersection point at $x_2^A \approx 0.85$. In particular, the noted A-dependence of u_i for which $B^D(u_i) = B^A(u_i)$ causes x_2^A to be larger for ^{4}He than for $A \gtrsim 12$. The same results from a relativistic PWIA calculation [43].

We mention here an entirely different approach, where one exploits a sum-rule for the nucleonic parts of the involved NI components of SF (cf. Eq. (3.2))

$$\int_0^A \frac{dx}{x} F_2^A - \int_0^2 \frac{dx}{x} F_2^D \approx \int_{x_0}^{x_U} \frac{dx}{x} \left[F_2^A - F_2^D \right] = 0 \ . \tag{3.6}$$

The approximations in Eq. (3.6) are based on the widths of $f^{PN,A}$ in the SFs, which effectively cut the supports of x, and allows the above upper and lower limits of integration to be replaced by common x_U, x_0. As a consequence the difference $F_2^A - F_2^D$ (and in fact $F_2^A - F_2^{A'}$, for any A, A') has to change sign at least once in the interval $0.20 \lesssim x \lesssim 0.90$ [44], or alternatively their ratio has to pass there through 1.

IV) Next we comment on the slopes $s^A(x, Q^2) = \partial \mu^A(x, Q^2)/\partial x$ at $x_{1,2}$. Eqs. (3.2) and (3.3) imply that all SFs and their slopes are about equal in some interval around the small $x \approx 0.2$, leading to a small negative, and nearly A-independent slope of EMC ratios around x_1. One estimates

$$s^A(x \approx x_1) \equiv \mu^A \left[\frac{\partial(\log F_2^A)}{\partial x} - \frac{\partial(\log F_2^D)}{\partial x} \right]\Bigg|_{x_1} \approx s(x \approx x_1) \approx -0.3 \ . \tag{3.7}$$

While F_2^A hardly depends on A for $x \approx x_2$, its slope $\partial F_2^A(x)/\partial x \big|_{x \approx x_2^A}$ does so strongly. Consequently, and in contrast to the same around $x \approx x_1$, $s^A(x \approx x_2^A)$ is positive and large, in agreement with observation [1, 42].

The above arguments locate the position of a minimum for constant slopes at $x_m \gtrsim (x_1 + x_2^A)/2 \approx 0.65$, about as observed. A more quantitative estimate for the actual value of $\mu^A(x, Q^2)$ at the minimum requires details of the x-variation of the slopes $s^A(x)$.

B. The immediate QE peak region $|x - 1| \lesssim 0.05$.

V) We already mentioned that for increasing x, the rapid fall-off of $F_2^{N,NI}(ux, Q^2)$ in the integral (2.2) requires $u \ll 0.8$, which Figs. 3 and 4 place in the elastic tails of $B^A(u)$. In that region $B^A > B^D$ and consequently $\mu^A \gg 1$.

Until this point we considered NI components, which virtually always dominate nuclear SF and thus the EMC ratios. However, around the QE peak $x \approx 1$ the NE components are relatively large, in particular for the lightest targets and for $Q^2 \lesssim (2.5 - 3.0)\,\mathrm{GeV}^2$. For a discussion of their role, it is convenient to introduce relative weights $\gamma^A = F_2^{A,NI}/F_2^{A,NE}$ in the total $F_2^A = F_2^{A,NI} + F_2^{A,NE}$ and additional auxiliary EMC ratios $\mu^{A,NI}, \mu^{A,NE}$ for pure NI and NE components of the contributing SF. One then finds

$$\mu^A = \mu^{A,NI} \frac{\left[1 + (\gamma^A)^{-1}\right]}{\left[1 + (\gamma^D)^{-1}\right]} , \tag{3.8}$$

$$\approx \mu^{A,NI} , \qquad Q^2 \gtrsim 4\,\mathrm{GeV}^2 ; \ x \lesssim 0.95 , \ x \gtrsim 1.05 , \tag{3.9}$$

$$= \mu^{A,NE} \frac{\left[1 + \gamma^A\right]}{\left[1 + \gamma^D\right]} , \tag{3.10}$$

$$\approx \mu^{A,NE} , \qquad Q^2 \lesssim (2.5 - 3.0)\,\mathrm{GeV}^2 ; \ |x - 1| \lesssim 0.05, \ x \gtrsim 1.25 \tag{3.11}$$

Eq. (3.9) states that, when dominant, NI components are hardly perturbed by NE. However, for $A \leq 4$ and $Q^2 \lesssim (2.5 - 3.0)\,\mathrm{GeV}^2$ one may have a reversed situation with $\gamma^A \ll 1$. In that case, Eq. (2.5) implies

$$\mu^A(x \approx 1, Q^2) \approx \mu^{A,NE}(x \approx 1, Q^2) = \frac{f^{PN,A}(x \approx 1, Q^2)}{f^{PN,D}(x \approx 1, Q^2)} \ll 1 , \tag{3.12}$$

roughly symmetric around $x \approx 1$, as is the case for the SF $f^{PN,A}$, see the discussion at point a) of Section IIIA. The sharp increase beyond the value 1 in μ^A for $x_2 \approx 0.85 - 0.90$, and for Q^2 in the above range, is thus followed by an equally abrupt decrease into a deep local minimum. The relative A-dependence of the minimum is read-off from Fig. 1

$$\mu^{\bar{A}}(x \approx 1) < \mu^{\mathrm{He}}(x \approx 1) \lesssim 1 , \tag{3.13}$$

For low Q^2, the depth of the minimum is ≈ 0.35 for $A \geq 12$, and only ≈ 0.50 for $A = 3, 4$.

As long as the NI admixtures in F_k^A are small (cf. Eq. (3.11)), the position of the minimum at $x \approx 1$ is only weakly dependent on Q^2, because the ratio (3.12) is so. For increasing Q^2, NI components grow rapidly relative to NE ones. As a result NI components are never completely negligible and compete, even when NE is maximal [34]. This affects the specific NE effect above: the narrow minimum at $x \approx 1$ is contaminated with NI components, and ultimately vanishes in an asymmetric way around $x = 1$. The resulting μ^A for sufficiently large Q^2 will show a practically smooth steep increase from $x \approx 0.85$ on (see Figs. 7,8,9,10).

C. The DQE region.

VI) Further increasing $x > 1$, one can no more have simultaneously an argument $xu \lesssim 0.8$ of $F_2^{\langle N \rangle}(xu, Q^2)$, in Eq. (2.3), and u in $B^A(u)$ anywhere close to 1. Consequently both small factors in the integrand combine to yield strongly reduced values for nuclear SF F_2^A (cf. Fig. 6). The crucial issue is a reliable prediction for the ratios $\mu^A = F_2^A/F_2^D$.

The approximation $\mu^A \approx \mu^{A,NE}$, Eq. (3.11) also holds for $x \gtrsim 1.25$, where NI components decrease faster in x, ultimately leading to NE$\gg$NI.

Figs. 4 and 5 show that for sufficiently small u all B^A decrease with a characteristic A-dependence. For fixed u, again the effect is most prominent for the D. Compared to it, the decrease is less, and about similar for He and Fe, and even smaller for the other targets considered. Comparison of Figs. 4,5 shows a clear Q^2-dependence. Consequently EMC ratios rapidly increase for $x \geq 1.05$ to values far in excess of 1 in an A and Q^2-dependent fashion.

This concludes a more than heuristic description. There is little doubt that the simple, outspoken x, A dependence of the SF $f^{PN,A}$ for a nucleus of point-nucleons describes all characteristic features of EMC ratios in the (deep)

inelastic classical regime $0.2 \lesssim x \lesssim 0.95$, through the QE region $0.95 \lesssim x \lesssim 1.05$, and up in x into the DEP region $1.05 \lesssim x \lesssim 1.4$. Actual quantifications of the above observations are obviously required.

We close this Section with a remark on generalized EMC ratios. Up to this point we dealt with EMC ratios of F_2^A and F_2^D. Similar considerations can be forwarded when comparing F_2^A with $F_2^{\langle N \rangle}$, the properly weighted SF of a nucleon. The situation is different for generalized EMC ratios $\mu^{A,A'}$, $A' \geq 12$, which from the above are seen to deviate from 1 by no more than a few % [48]. Again the He isotopes occupy a special position. For instance in the classical regime $|1 - \mu^{A,^4\text{He}}| < |1 - \mu^{A,^3\text{He}}| < |1 - \mu^{A,D}|$. Indeed, data on EMC ratios $\mu^{A,^3\text{He}}$ show all features of $\mu^{A,D}$, but in a more temperate fashion [49].

IV. INPUT, RESULTS.

In the following we present computed EMC ratios, which should underscore the above qualitative considerations. We start with some input elements.

a) SFs $f^{PN,A}$ for nuclei composed of point-nucleons can only be computed with great precision for the lightest nuclei [32, 33]. For heavier nuclei approximations are unavoidable and we used the one discussed in Ref. [30]. For all A we calculated $f^{PN,A}(x, Q^2)$ from a related function $\phi^A(y_G, |\boldsymbol{q}|)$ defined in terms of different kinematic variables, namely $|\boldsymbol{q}|$, the 3-momentum transfer, and y_G, the Gurvitz scaling variable [50], which is typical for the underlying, non-perturbative method (see Ref. [30])

$$y_G^A = \frac{2y_G}{1 + \sqrt{1 + 2\nu y_G/(M_{A-1}|\boldsymbol{q}|)}} \, , \tag{4.1}$$

$$y_G = M\nu/|\boldsymbol{q}|[1 - \langle\Delta\rangle/M - x] \, , \tag{4.2}$$

$$\delta(x) \approx -\frac{\delta\langle\Delta\rangle}{M} \, . \tag{4.3}$$

Above, y_G^A for a recoiling spectator nucleus with finite mass M_{A-1} is in Eq. (4.1) expressed in terms of the same, Eq. (4.2), for an infinite mass spectator. Only for the lightest nuclei does one have to retain the recoil correction in Eq. (4.1) [28, 33].

In expression (4.2) appears an average separation energy of a nucleon in the target, which for ^{4}He, C, Fe, Au we took as $\langle\Delta\rangle = 20.2, 40, 45, 45$ MeV. Eq. (4.3) expresses for given y_G the change in x, due to the same in $\langle\Delta\rangle$. The above is important if $f^{PN,A}$ varies rapidly with x, i.e. in the neighborhood of $x = 1$. A consequence of this fact will be shortly encountered.

b) Since for all applications $Q^2 \geq 3.5$ GeV^2, we employ for F_2^p a parametrization of resonance-averaged data [40], instead of one for F_2^p itself for $Q^2 \lesssim (4.0 - 4.5)$ GeV^2 [51].

c) F_k^n is not-directly accessible and we follow a previously introduced method for its extraction from inclusive scattering data on targets, where neutrons are bound [52]. There one parametrizes the ratio

$$C(x, Q^2) = F_2^n(x, Q^2)/F_2^p(x, Q^2) = \sum_{k=0}^{2} d_k(Q^2)(1 - x)^k \tag{4.4}$$

and determines a minimal set of parameters in Eq. (4.4) from the known values $C = 1$ for $x = 0$ and $C = 0.75$ for the small $x = 0.2$, for which the primitive relation (3.1) holds. Beyond the lowest inelastic threshold, $C(x, Q^2) = 0$, except at the physical boundary $x = 1$, where C depends solely on static form factors

$$C(x = 1, Q^2) = \frac{\left(G_E^n(Q^2)\right)^2 + \eta\left(G_M^n(Q^2)\right)^2}{\left(G_E^p(Q^2)\right)^2 + \eta\left(G_M^p(Q^2)\right)^2} \, . \tag{4.5}$$

The form factors above are those advocated in [53] from cross section data (see also Ref. [22]).

At this point we remark on extracted EMC ratios. For relatively low Q^2 those are overwhelmingly from SLAC NE3 data [8], and those have been discussed before [3, 4, 5, 9]. We therefore limit ourself to EMC ratios extracted from JLab E89-008 data with $Q^2 \gtrsim 3.5$ GeV^2 [13], and to which the remarks at the end of a) in this Section apply: A proper analysis of those data for fixed scattering angles θ, for which Q^2 varies with x, requires an interpolation to a few given Q^2, but there are not enough data points to do so reliably. In the end we performed computations for

A=D, ^{4}He, C, Fe, Au at fixed $Q^2 = 3.5, 5.0, 10$ GeV^2 and $0.2 \lesssim x \lesssim 1.5$. Actually shown data points for $x \gtrsim 1.1$ may well differ by $\lesssim 10\%$ from those for the above fixed Q^2.

Here we pose the question, which F_2^D should be used in the denominator of μ^A. Off-hand it seems best to use experimental values. Nevertheless we advocate the computed F_2^D, which has been calculated in the same approach for all F_2^A. Those carry therefore the same 'systematic' imperfections which may partly cancel in ratios. The choice is of minor practical relevance, since the computed F_2^D agree well with the parametrized resonance-averaged data [40].

In Figs. 7,8,9,10 we display data and computed EMC ratios for ^{4}He, C, Fe and Au, at $Q^2 = 3.5, 5.0, 10.0$ GeV^2 over two separated ranges $0.2 \lesssim x \lesssim 0.90$ and $x \geq 0.80$ with different vertical scales. For the classical range we used the original data from Refs. [45, 46, 47] (open circles), while revised results and additional data [54, 55] are given as closed circles. Occasionally we use averages as compiled in Ref. [42]. In all figures, bars on data points refer only to statistical errors. One finds confirmed the near-insensitivity to Q^2, except for $Q^2 = 3.5$ GeV^2: Ratios of slightly irregular F_2^A cause some structure in predictions around $x = 0.7$.

In the DI region there is reasonable, but not perfect agreement. At the QE peak $x = 1$, data show noticeable inelastic NI effects on the NE ratios $\mu^{A,NE}$, Eq. (3.13). Beyond, for $x \geq 1.0$ we show extracted data for actual, non-interpolated $Q^2 = (3.4 - 4.2)$ GeV^2, marked by empty squares (see also Refs. [3, 4, 5]). Those extracted for $Q^2 = (4.5 - 5.3)$ GeV^2 are shown as filled squares. Theoretical curves are for fixed $Q^2 = 3.5$, respectively 5.0 GeV^2.

In the DQE region all data show a strong Q^2 and a much more tempered A-dependence, which computations follow to within better than $\approx 15\%$, except for the largest x for Fe. A glance at Fig. 1 shows that barely visible changes in the tail can easily make up for, or increase the difference. In detail:

^{4}He: no data; predicted is a maximum with a subsequent decrease.

C: Predictions follow the steep increase of the data, but fall short of them by about 15%.

Fe: As for C, but the data (with large error bars!!) continue to increase for $x \gtrsim 1.25$, whereas calculations for $Q^2 \leq 5$ GeV^2 show a leveling-off.

Au: Good agreement. No data beyond $x \approx 1.25$, where theory predicts maxima for all Q^2.

Given the sensitivity and small numbers involved, also the agreement in the DQE region to $x \approx 1.2$ is satisfactory. In fact all results are much in line with the spelled-out, qualitative predictions with regard to intersection points, minima in the classical regime, including their A-dependence, the structure and Q^2-dependence of the minima around $x = 1$ and a subsequent increase beyond. In both regimes $\mu^{^4\mathrm{He}}$ is clearly different from other μ^A. For the He isotopes, the presently running Jlab EMC experiment E03-103 will provide a test for the Q^2-dependence of μ^A, in particular for the predicted gradual fading of the minimum at $x = 1$ for increasing Q^2.

V. DISCUSSION, COMPARISON AND CONCLUSION.

In the present note we have studied nuclear SFs F_2^A, F_2^D and their EMC ratios over the kinematic range $0.2 \lesssim x \lesssim 1.5$. All along we have been aware that both composing nuclear SFs in those ratios decrease two orders of magnitude between $x \approx 0$ ($F_2^A \approx 0.37$) and $x \approx 1$. In that interval the EMC effect, i.e. the deviations of EMC ratios from 1 are less than 20% and on the average 10%. The above requires the accuracy of the computed ratios to be better than the size of EMC effect.

Further increasing x to about 1.4-1.5, the involved SF decrease by another two orders of magnitude and it seems extremely hard to fulfill even far less stringent requirements than imposed on the classical region. The above has not deterred attempts to compute EMC ratios.

The tool of our analysis has been a postulated relation between nuclear and nucleon SFs, linked by $f^{PN,A}$, the SF of an unphysical nucleus, composed of point-particles. The computation of the latter requires many-particle density matrices, diagonal in all nuclear coordinates except one, which are constructed from nuclear ground state wave functions. Such a calculation is presently only feasible for the D and the He isotopes and approximate methods had to be invoked for $A \geq 12$. In addition one needs information and models for off-shell NN elastic scattering.

Calling on characteristic properties of $f^{PN,A}$ as function of x, Q^2 and A and on the x, Q^2-dependence of the properly weighted nucleon SF $F_2^{\langle N \rangle}$, we first qualitatively accounted for all characteristic features of EMC ratios in the classical regime $0.2 \lesssim x \lesssim 0.95$, the QE peak area $0.95 \lesssim x \lesssim 1.05$, and continuing into the DQE region $1.05 \lesssim x \lesssim 1.4$, including the A dependence of μ^A. The same considerations carry over to generalized EMC ratios $\mu^{A,\mathrm{He}}$, in particular for ^{3}He, and recent data for the latter confirm those [49].

The above qualitative considerations lead only to ordering of relevant quantities, or alternatively, to inequalities. In the end we performed actual calculations of EMC ratios to underscore the above qualitative considerations. It is not surprising that, contrary to the reliable, qualitative considerations, the very small values of the SF involved do not guarantee a similar accuracy in directly calculated results. Nevertheless we obtained reasonable agreement with data in the classical regime $0.2 \lesssim x \lesssim 0.9$ and beyond, with extracted EMC ratios for $0.9 \lesssim x \lesssim 1.25$.

The emphasis above has been on an explanation solely based on the properties of the SFs $f^{PN,A}$ and $F_2^{\langle N \rangle}$: We are not aware of an alternative simple description, which is not a judgment against other approaches. We re-assert the obvious: In principle, 'complete' treatments of various approaches to nuclear SF produce identical results. However, in practice theories are worked out to some order in a parameter, which is characteristic for the chosen approach. An issue emerges when comparing two results in two approaches to *different* orders in *different* parameters.

At this point we recall a proof, explicitly showing that the GRS and DWIA approaches produce similar results if both are compared to the *same* order in a common expansion parameter, e.g. the lowest order in NN re-scattering [56]. It does therefore not come as a surprise to find similar agreement for EMC ratios, computed in the afore-mentioned two theories.

In spite of the above, it is of interest to note different insights in some aspects of EMC ratios, for instance around the minima in $\mu^A (x \approx 1)$. The DQE region $x \gtrsim 1$ has repeatedly been discussed [3, 4], with as most complete treatment (essentially a DWIA), the one by Benhar *et al* [5]. No particular role is allocated there to the QE point. In fact the earlier treatment by Frankfurt *et al.* [3] allocates the above to the ratio of the longitudinal momentum distributions. In order to reach that result in the DWIA, one has first to neglect FSI, which indeed are relatively small around the QEP. However, in order to reach the longitudinal momentum distribution from the PWIA, one has to concentrate the spread of the spectral function into one peak. The cited steps are not manifestly equivalent to the dominance of the NE contributions in the GRS approach and its consequences. One would also have to show that the above ratio of Q^2-independent longitudinal momentum distribution equals the Q^2 dependent ratio of $f^{PN,A}(x \approx 1, Q^2)$.

Our last remark regards the treatment of the DQE region. For relatively low Q^2, the EMC ratios have mostly been extracted from F_2^A (SLAC NE3 experiment [8]) against F_2^D and from a single recent experiment of the same against $F_2^{^3\text{He}}$ [49]. Those data show that, after an initial increase, the EMC ratios μ^A ultimately reach plateaux of approximately constant values. For increasing Q^2, Eq. (3.11) is no more valid. As a consequence EMC ratios continue to raise, possibly reaching a plateau at a much larger x.

In a very simplistic description the appearance of the latter at lower Q^2 have been interpreted as due to correlations between the struck and 2,3... spectator particles [3]. It is clearly of interest to see whether such a chain of approximations applied to the GRS expressions lead to the above-mentioned simple result. Those steps will be elaborated in a separate note.

In conclusion, we continue to be amazed and do not fully understand, why theoretical EMC ratios appear to agree with data out to large x, where each participating nuclear SF is extremely small. It is hard to believe that the relative uncertainties in the participating F_2^A are practically A-independent and cancel in EMC ratios. To our opinion, understanding the above remains a challenge.

VI.   ACKNOWLEDGMENT.

[1] M. Arneodo, Phys. Reports 240, 301 (1994).
[2] D.F. Geeseman, K. Saito and A.W. Thomas, Ann. Rev. Nucl. Part, Sci. 45, 337 (1995).
[3] L.L. Frankfurt, M.I. Strikman, D.B. Day and M. Sargsyan, Phys. Rev. C 48, 2451 (1993).
[4] S. Liuti, Phys. Rev. C 47, 1854 (1993).
[5] O. Benhar, A. Fabrocini, S. Fantoni and I. Sick, Phys. Lett. B 343, 47 (1995).
[6] D. Day *et al.*, Phys. Rev. Lett. 43, 1143 (1979).
[7] S. Rock *et al.*, Phys. Rev. C 26, 1592 (1982).
[8] D. Day *et al.*, Phys. Rev. C 48, 1849 (1993).
[9] P.E. Bosted *et al.*, Phys. Rev. Lett. 68, 3841 (1992).
[10] S. Rock *et al*, Phys. Rev. Lett. 49, 1139 (1982).
[11] R.G. Arnold *et al.*, Phys. Rev. Lett. 61, 806 (1988).
[12] W.P. Schuetz *et al.*, Phys. Rev. Lett. 38, 250 (1977).
[13] J. Arrington *et al.*, Phys. Rev. Lett. 82, 2056 (1999): J. Arrington, PhD Thesis Cal.Tech, 1998.
[14] J. Arrington *et al.*, Phys. Rev. C 64, 014602 (2001).
[15] I. Niculescu *et al.*, Phys. Rev. Lett. 85, 1182 (2000).
[16] S.D. Ellis and W.J. Stirling, Phys. Lett. B 256, 258 (1991).
[17] C. Ciofi delgi Atti, E. Pace and G. Salme, Phys. Rev. C 43, 1155 (1991).
[18] C. Ciofi delgi Atti and S. Liuti, Phys. Rev. C 41, R1269 (1991).
[19] O. Benhar *et al.*, Phys. Rev. C 44, 2328 (1991).

[20] P. Fernandez de Cordoba, E. Marco, H. Muether, E. Oset and A. Faessler, Nucl. Phys. A 611, 514 (1996).
[21] J.R. Smith and G.A. Miller, Phys. Rev. Lett. 91, 212301 (2003).
[22] J. Arrington, R. Ent, C.E. Keppel, J. Mammei and I. Niculescu, [arXiv: nucl-ex/0307012].
[23] S.A. Akulinichev, S. Shlomo, S. Kulagin and G.M. Vagradov, Phys. Rev. Lett. 55, 2239 (1985).
[24] J. Rozynek and G. Wilk, [arXiv:hep-ph/0211320].
[25] A. Molochkov, [arXiv:nucl-th/0407077].
[26] J. Arrington, D. Gaskell *et al.*, Jlab E03-103 experiment.
[27] S.A. Gurvitz and A.S. Rinat, TR-PR-93-77/ WIS-93/97/Oct-PH; Progress in Nuclear and Particle Physics, Vol. 34, 245 (1995).
[28] S.A. Gurvitz and A.S. Rinat, Phys. Rev. C 65, 024310 (2002).
[29] H. Gersch, L.J. Rodriguez and Phil N. Smith, Phys. Rev. A 5, 1347 (1973).
[30] A.S. Rinat and M.F. Taragin, Nucl. Phys. A 598, 349 (1996).
[31] A.S. Rinat and M.F. Taragin, Nucl. Phys. A 620, 412 (1997); Erratum: *ibid* A623, 773 (1997); Phys. Rev. C 60, 044601 (1999).
[32] A.S. Rinat and M.F. Taragin, Phys. Rev. C 65, 042201(R) (2001).
[33] M. Viviani, A. Kievsky and A.S. Rinat, Phys. Rev. C 67, 034003 (2003).
[34] A.S. Rinat, M.F. Taragin and M. Viviani, Phys. Rev. C 70, 014003 (2004), and ms. submitted to Phys. Rev. C. [arXiv:nucl-th/0410100].
[35] A.S. Rinat and M.F. Taragin, Phys. Rev. C 62, 034602 (2000). 034602 (2000).
[36] C.H. Llewelyn Smith, Phys. Lett. B 128 (1983) 107; M. Ericson and A.W. Thomas, *ibid* p. 112.
[37] G. Piller and W. Weise, Phys. Report 330, 1 (2000).
[38] G.B. West, Ann. of Phys. (NY) 74, 646 (1972); W.B. Atwood and G.B. West, Phys. Rev. D 7, 773 (1973).
[39] M.M. Sargsian, S. Simula and M.I. Strikman, Phys. Rev. C 66, 024001 (2002).
[40] M. Arneodo, Phys. Lett. B 364, 107 (1995).
[41] S. Akulinitchev, S.A. Kulagin and G.M. Vagradov, Phys. Lett. B 158, 485 (1985).
[42] J. Gomez *et al.*, Phys. Rev. D 49, 4348 (1994).
[43] V.V. Burov, A.M. Molochov, G.I. Smirnov, Phys. Lett. B 466, 1 (1999).
[44] A.S. Rinat and M.F. Taragin, in preparation.
[45] P. Amadrauz *et al.*, Nucl. Phys. B 441, 3,12 (1995).
[46] J. Ashman *et al.*, Nucl. Phys. B 202, 603 (1988); M. Arneodo *et al* Nucl. Phys. B 333, 1 (1990).
[47] A. Bodek *et al.*, Phys. Rev. Lett. 50, 1431 (1983); A.C. Benvenuti *et al* Phys. Lett. B 189, 483 (1987); S. Dasu *et al.*, *ibid.* 60, 2591 (1988).
[48] M. Arneodo *et al.*, Nucl. Phys. B 481, 23 (1988).
[49] K.Sh. Egiyan *et al.*, Phys. Rev. C 68, 014313 (2003).
[50] S.A. Gurvitz, Phys. Rev. C 42, 2653 (1990).
[51] E. Christy *et al.*, Phys. Rev. C 70, 015206 (2004).
[52] A.S. Rinat and M.F. Taragin, Phys. Lett. B 551, 284 (2003).
[53] H. Budd, A. Bodek and J. Arrington, [arXiv:hep-ex/0308005].
[54] G. Bari *et al*, Phys. Lett. B 163, 282 (1085).
[55] P. Amadrauz *et al*, Zeitschr, f. Physik C 51, 387 (1991).
[56] A.S. Rinat and B. Jennings, Phys. Rev. C 59, 3371 (1999).

TABLE I: Target ordering of $B^A(u,Q^2)$, Eq. (2.5), as function of u,Q^2. The same for nuclear SF $F_2^A(x,Q^2)$ and EMC ratios $\mu^A(x,Q^2)$ as function of x,Q^2 (Q^2 is in units GeV^2). When not distinguishing between different targets, we just use A.

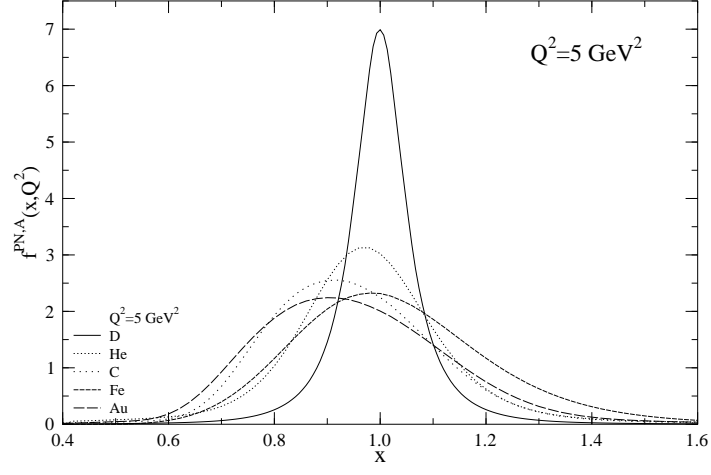| Function ordered targets	u,x interval	u,x interval	u,x interval	u,x interval
	$0.6 \leq u \leq 0.9$	$0.95 \leq u \leq 1.05$	$1.05 \leq u \leq 1.1$	$u \geq 1.1$
$B^A(u,Q^2 \leq 10)$	A $\gg$ D	D $\gg$ He > A	He > A $\gg$ D	A > He $\gg$ D
	$0.4 \leq x \leq 0.8$	$0.85 \leq x \leq 0.95$	$0.95 \lesssim x \lesssim 1.05$	$1.1 \lesssim x \lesssim 1.5$
$F_2^A(x, 3.5 \div 5.0)$	D > He > C $\gtrsim$ Fe	D $\gtrsim$ A	C > He $\approx$ Fe $\gg$ D	C > Fe, He $\gg$ D
$F_2^A(x, 10.0)$	D > He > C $\gtrsim$ Fe	C > He > Fe $\gg$ D	C > He > Fe $\gg$ D	C $\gg$ He, Fe $\gg$ D
	$0.3 \lesssim x \lesssim 0.75$	$0.85 \leq x \leq 0.95$	$0.95 \lesssim x \lesssim 1.05$	$x \gtrsim 1.05$
$\mu^A(x, 3.5)$	1 > He > A > Fe	He $\gtrsim$ A > 1	C > He > A	C > A > Au
$\mu^A(x, 5.0)$	1 > He > A > Fe	He $\gtrsim$ A > 1	C > He > A	C $\gg$ A > He
$\mu^A(x, 10.0)$	1 > He > A > Fe	He $\gtrsim$ A > 1	C > He > A	C $\gg$ A > Fe
$Q^2 = 3.5$	1 > μ^{He} > μ^A > μ^{Fe}	μ^{He} > μ^A > 1	μ^C > μ^{He} > μ^A	μ^C > μ^A > μ^{Au}
$Q^2 = 5.0$	1 > μ^{He} > μ^A > μ^{Fe}	μ^{He} > μ^A > 1	μ^C > μ^{He} > μ^A	μ^C $\gg$ μ^A > μ^{He}
$Q^2 = 10.0$	1 > μ^{He} > μ^A > μ^{Fe}	μ^{He} > μ^A > 1	μ^C > μ^{He} > μ^A	μ^C $\gg$ μ^A > μ^{Fe}

FIG. 1: The point-nucleon nuclear SF $f^{PN,A}(x,Q^2)$ for D, ^{4}He, Fe, C and Au; $Q^2 = 5\,\mathrm{GeV}^2$.
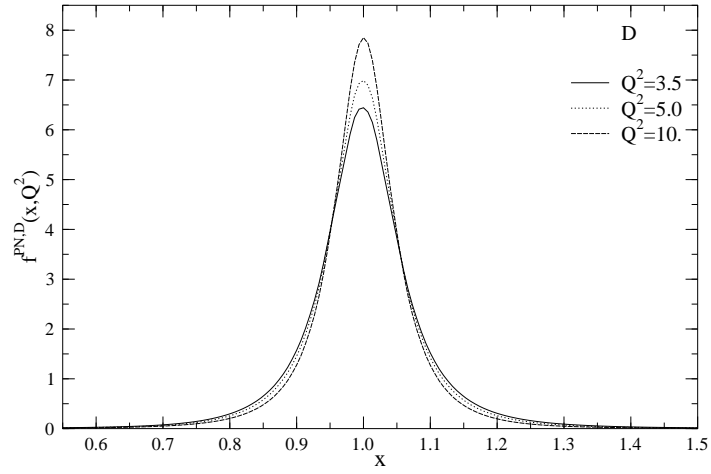

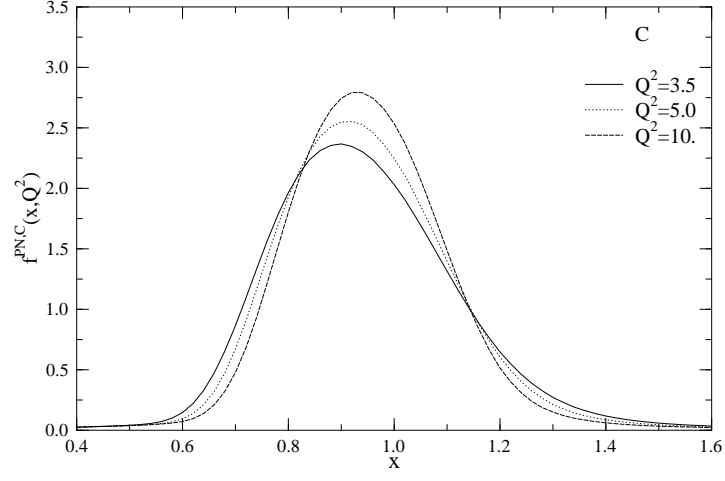FIG. 2: Same as Fig. 1 for D; $Q^2 = 3.5, 5, 10\,\mathrm{GeV}^2$.

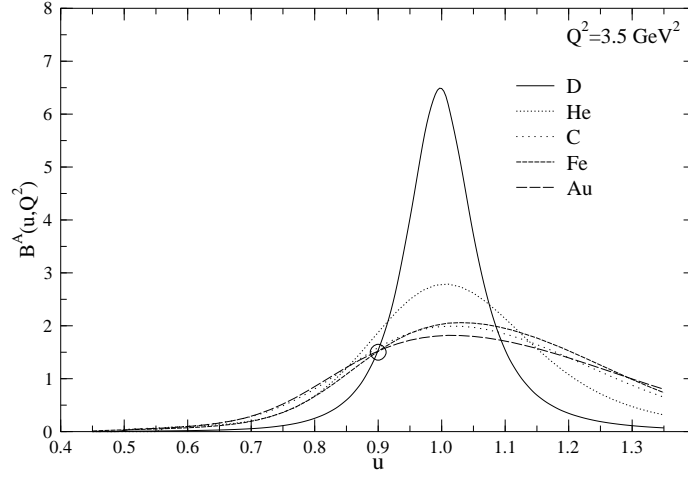FIG. 3: Same as Fig. 1 for C; $Q^2 = 3.5, 5, 10 \, \text{GeV}^2$.

FIG. 4: The function $B^A(x, Q^2)$, Eq. (2.3) for our chosen targets; $Q^2 = 3.5 \text{GeV}^2$. The circles mark the nearly identical crossing point u_i^A for D and $A > 4$, different from the same for ^4He and D.
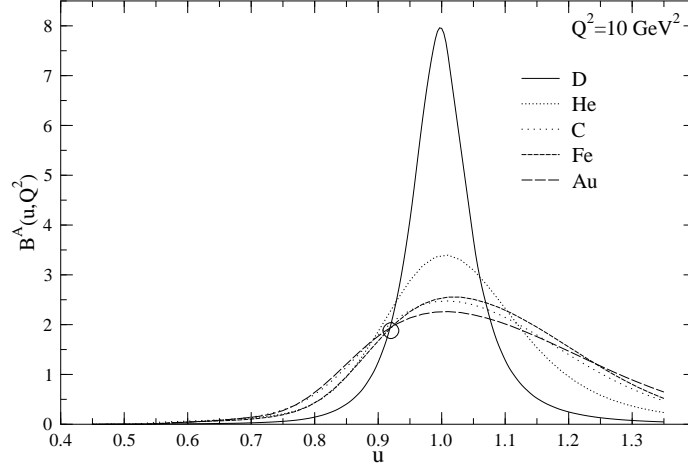
FIG. 5: Same as Fig.4; $Q^2 = 10$ GeV^2.
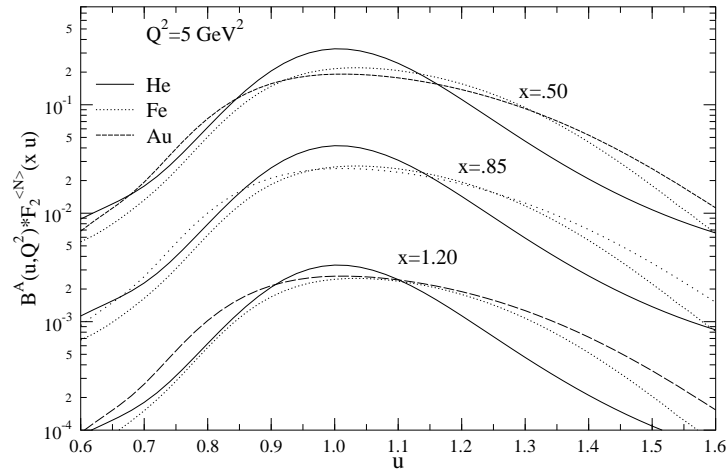
FIG. 6: The integrand $B^A(x, Q^2)F_2^{\langle N \rangle}(xu, Q^2)$ in Eq. (2.2), which determines the size of the integrals for F_2^A, for He, Fe, Au (drawn, dotted and dashed lines) and fixed $Q^2 = 5.0$ GeV^2. The sets of curves show, that the above products decrease about a factor of 10 for increasing $x = 0.5 \rightarrow 0.85 \rightarrow 1.2$.
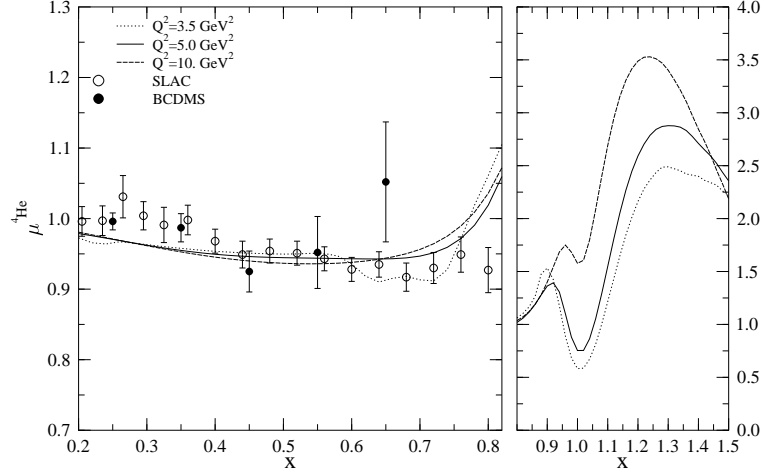
FIG. 7: $\mu^{^4\text{He}}$ for $Q^2 = 3.5, 5.0, 10.0, \text{GeV}^2$. Data in the classical range are from Ref. [42] (open circles) and Ref. [45] filled circles. No extracted data exist beyond that range.
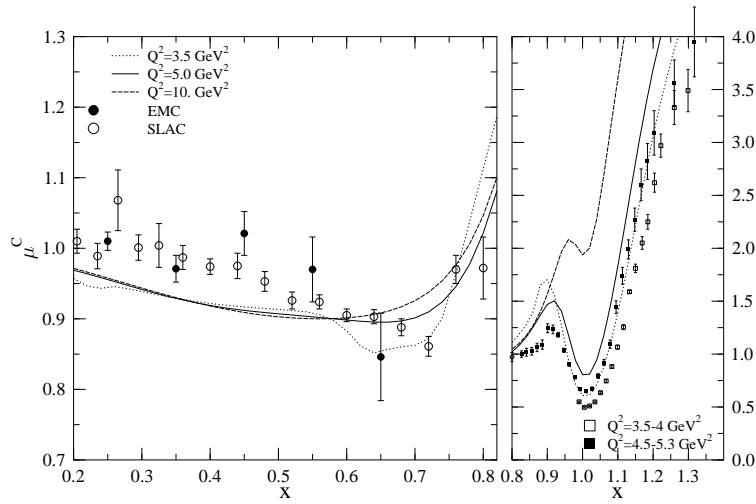

FIG. 8: Same as Fig. 7 for μ^{C}. Data sets in the classical range are from Refs.[42, 46]. Extracted data are for varying $Q^2 \approx 3.4 - 4.2 \, \text{GeV}^2$ (open diamonds) and for varying $Q^2 \approx 4.5 - 5.2 \, \text{GeV}^2$ (filled diamonds) [14, 15]. Data are too sparse for interpolation towards $Q^2 = 3.5$ and $5.0 \, \text{GeV}^2$ for which calculated results are presented.
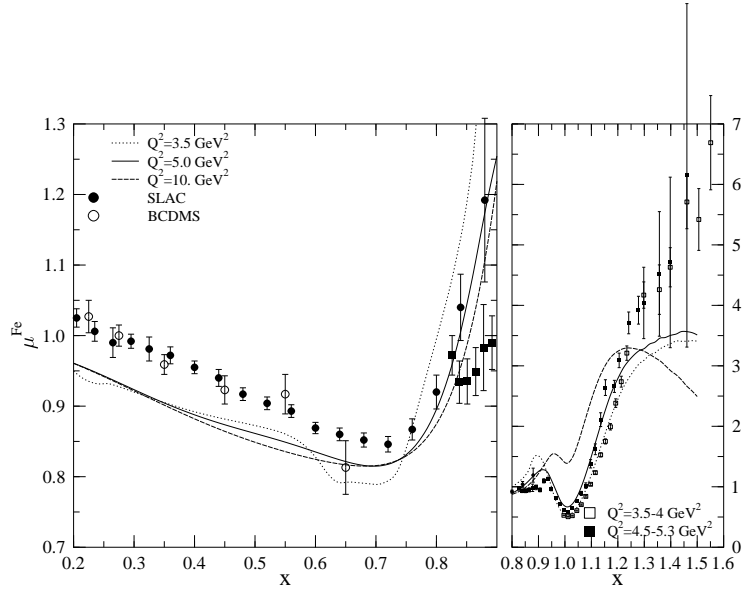
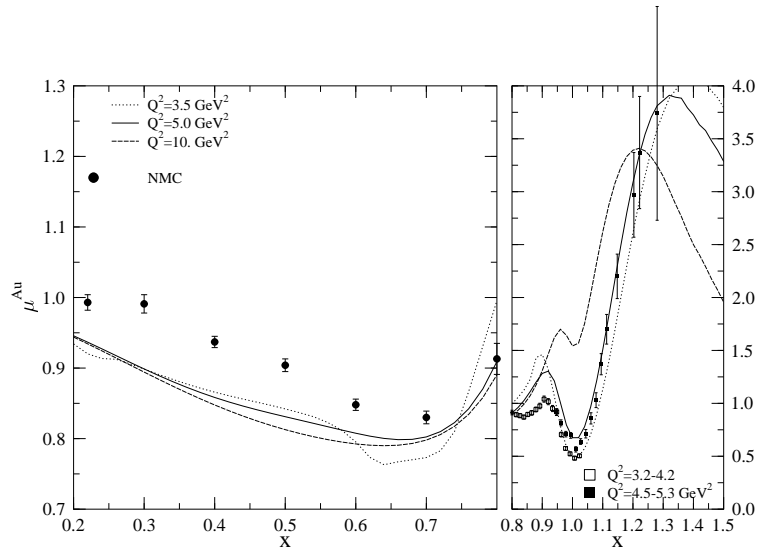FIG. 9: Same as Fig. 7 for μ^{Fe} (Data from Refs. [42, 47]; see text in Section IV).

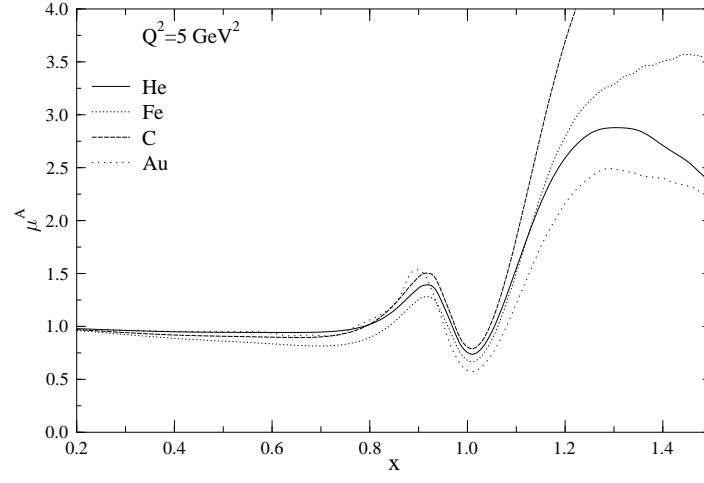FIG. 10: Same as Fig. 7 for μ^{Au} (Data from Ref. [42]; see text in Section IV).

FIG. 11: A-dependence of computed EMC ratios.